

See discussions, stats, and author profiles for this publication at: <https://www.researchgate.net/publication/361408449>

Higher-Order Sliding Mode Design With Bounded Integral Control Generation

Article in *Automatica* · September 2022

DOI: 10.1016/j.automatica.2022.110430

CITATIONS

2

READS

123

3 authors:



Antonio Russo

Università degli Studi della Campania "Luigi Vanvitelli"

29 PUBLICATIONS 171 CITATIONS

[SEE PROFILE](#)



Gian Paolo Incremona

Politecnico di Milano

88 PUBLICATIONS 1,660 CITATIONS

[SEE PROFILE](#)



Alberto Cavallo

Università degli Studi della Campania "Luigi Vanvitelli"

169 PUBLICATIONS 1,568 CITATIONS

[SEE PROFILE](#)

Some of the authors of this publication are also working on these related projects:



HYPNOTIC [View project](#)



Advanced Control Strategies for Electric Power Management, Special Issue of ENERGIES Journal (ISSN 1996-1073) IF: 2.702 [View project](#)

Higher-Order Sliding Mode Design With Bounded Integral Control Generation ^{★★}

Antonio Russo ^a, Gian Paolo Incremona ^{b,*}, Alberto Cavallo ^a

^a*Dipartimento di Ingegneria, Università degli Studi della Campania “L. Vanvitelli”, 81031 Aversa, Italy*

^b*Dipartimento di Elettronica, Informazione e Bioingegneria, Politecnico di Milano, 20133 Milan, Italy*

Abstract

In this paper uncertain continuous-time nonlinear systems affine in the control variable and with saturated actuators are considered. The finite-time regulation problem of the system output to zero is then solved by proposing a generic Higher-Order Sliding Mode (HOSM) controller equipped with a novel mechanism to encounter the saturation limits, thus extending previous results on saturated control inputs valid only in case of specific r -order sliding mode algorithms. The so-called Bounded Integral Control (BIC) method is reformulated into the framework of continuous HOSM, so as to replace the traditional integrator used to generate the continuous signal directly fed into the plant. Stability conditions for tuning the proposed algorithm are provided, and a numerical example finally assesses the effectiveness of the proposed technique.

Key words: Higher-order sliding mode, bounded input, integral control, nonlinear systems.

1 Introduction

Saturation constraints on the actuators are basically encountered in all real control problems, and their presence is a core issue leading to different theoretical and practical challenges [1, 2]. In fact, operational limits are naturally intrinsic or purposely imposed for reducing energy consumption, minimizing wear and tear of the plants, or avoiding bulky and expensive devices. Typical examples of systems with hard input and state constraints are power systems, transportation or robotic plants [3–5].

* This work has been partially supported by CleanSky2, grant Program H2020-CS2-CFP10-2019-01 JTI-CS2-2019-CfP10-SYS-02-59, Proposal 886559 HYPNOTIC, and by the Italian Ministry for Research in the framework of the 2017 Program for Research Projects of National Interest (PRIN), grant no. 2017YKXYXJ.

★★This is the authors' version of an article that has been published in *Automatica*. Changes were made to this version by the publisher prior to publication. The final version of record is available at

<https://doi.org/10.1016/j.automatica.2022.110430>

* Corresponding author: Politecnico di Milano, Piazza Leonardo da Vinci, 32 - 20133 Milano (Italy).

Email addresses: antonio.russo1@unicampania.it (Antonio Russo), gianpaolo.incremona@polimi.it (Gian Paolo Incremona), alberto.cavallo@unicampania.it (Alberto Cavallo).

In recent years, constrained dynamical systems have obtained an increasing interest and many approaches have been proposed in the literature to cope with them. However, in general, it is not easy to explicitly take into account constraints on the control input, and the presence of saturated actuators when an integral action is applied can imply the so-called integral windup phenomenon, i.e., undesired large and poorly decaying overshoots in transients during which the controller output can no longer affect the controlled variable [6]. Among the possible solutions to this issue, [7] presents a BIC algorithm capable of generating an integral control action which is bounded independently of the plant parameters and states. An enhanced version of this algorithm is instead proposed in [8], where a better approximation of the traditional integral action is provided by relaxing some restrictive hypotheses of the original technique.

Encountering actuator saturation can be even more challenging when unavoidable modeling uncertainties and disturbances affect the controlled systems. In fact, the saturation represents an additional nonlinearity to cope with, so that robust saturated control strategies can be valid solutions. In this context Sliding Mode Control (SMC) approaches perfectly fit to solve this problem [5, 9]. In particular, in this work we deal with the so-called continuous HOSM control algorithms designed starting from systems with generic relative degree ρ ,

adding an integrator dynamics in order to design a discontinuous HOSM control of order $r = \rho + 1$ (e.g., the continuous version of Twisting [10], Suboptimal [11], and Terminal [12] algorithms). These algorithms can provide beneficial effects in terms of chattering alleviation. Nevertheless, the presence of an additional integral dynamics *a priori* prevents the possibility to bound the effective continuous control signal, thus possibly implying a control amplitude which overcomes the intrinsic saturation of the system.

1.1 Contributions with respect to the state of the art

In this paper, to the best of the authors' knowledge, we present a novel design framework for continuous HOSM controllers embedding actuator saturation. We propose an alternative solution to the conventional saturated integrator, which typically requires additional anti-windup techniques (e.g., back calculation or clamping), while not providing any stability guarantee. Differently, one of the key features of our proposal is the intrinsic anti-windup property, for which we provide a rigorous stability proof for the controlled system. To pursue this objective, the HOSM control law is coupled with a novel mechanism relying on the BIC algorithm, which is originally recast in the sliding mode framework. The BIC mechanism plays here the role of the traditional saturated integrator capable of generating the continuous input to be sent to the plant, while fulfilling the saturation limits.

Relying on SMC theory, one of the contributions of our work is the extension of the family of HOSM algorithms applicable to systems with saturated actuators. This problem has been indeed previously solved in the literature in a custom way for each algorithm (see e.g., [13–18]), where a modification of the original version of the control strategies has been correspondingly proposed. For instance, [14] proposes a switching law for a Suboptimal algorithm based on the sign of the effective control input fed into the plant compared with its bounds. In [13, 16], Lyapunov based stability conditions are instead provided to maintain the input within saturation limits in the case of a Super-Twisting approach. Analogously, the recent work [17] exploits the conditioning technique, while in [19] a Lipschitz continuous saturated controller based on a Proportional-Integral (PI) control and a Twisting algorithm is proposed. In this paper, as an alternative, we introduce a well structured and rigorous method to account for actuator saturation that can be applied to any sliding mode controller of generic order r . The approach encompasses in a seamless way the use of saturation for continuous higher-order sliding mode controllers, which in general needs to be addressed with different and dedicated approaches.

Finally, making reference to the BIC theory in [7, 8], in this work, the BIC approach is deeply revised. Indeed,

while in [8] the BIC replaces the classical integral controller in the closed loop, in this paper it is embedded in the HOSM control law giving rise to a novel extended algorithm fulfilling input constraints. The revised approach allows to extend the BIC to the case of asymmetric saturation limits, among the contributions. Further, the new BIC structure enables finite-time convergence of its state trajectory towards the BIC characteristic curve, differently from [7, 8] where asymptotic convergence is shown. This result is here rigorously proved by using an approach based on a different Lyapunov function candidate. Moreover, the stability properties of the resulting saturated continuous HOSM control with BIC are thoroughly proved and assessed on a numerical example. It is worth to highlight that, without increasing the computational complexity, and with a simple design procedure relying on HOSM controllers in its original version, we achieve performance comparable with those resulting from customized, possibly more complex, structures of HOSM control laws in the case of saturating actuators.

1.2 Structure of the paper

In Section 2 the relevant notation is reported, while the problem formulation is introduced in Section 3. In Section 4 the proposed approach is presented and then analyzed in Section 5. A numerical example is illustrated in Section 6, and conclusions are drawn in Section 7.

2 Notation

Let \mathbb{R} be the set of reals, \mathbb{R}^+ be the set of positive reals, \mathbb{N} be the set of positive real integers, and $|\cdot|$ be the Euclidean norm. Given a column vector $v \in \mathbb{R}^n$, its transpose is given by v^\top . Given the function $g(z)$ and the vector field $f(z)$ sufficiently smooth, let $L_f g(z) := \frac{\partial g}{\partial z} f(z)$ be the so-called *Lie Derivative* of g along f . Finally, denote $\lfloor g \rfloor^q := |g|^q \operatorname{sgn}(g)$, with $q \in \mathbb{R}^+$ and $\operatorname{sgn}(g) = 1$ if $g > 0$, $\operatorname{sgn}(g) \in [-1, 1]$ if $g = 0$, and $\operatorname{sgn}(g) = -1$ if $g < 0$.

3 Problem formulation

Consider a plant (process and actuator) described by the single-input system affine in the control variable

$$\begin{cases} \dot{x}(t) = a(x(t)) + b(x(t))u(t) \\ y(t) = c(x(t)) \end{cases} \quad (1)$$

where $x \in \mathcal{D} \subset \mathbb{R}^n$ is the state vector, the value of which at the initial time instant $t_0 = 0$ is $x(0) = x_0$, and u is a Lipschitz continuous scalar input, subject to

$$u(t) \in \mathcal{U}, \quad \forall t \geq 0, \quad (2)$$

with $\mathcal{U} := [u_{\min}, u_{\max}] \subset \mathbb{R}$ being a compact connected set containing zero, with $u_{\min}, u_{\max} \in \mathbb{R}$ being the lower

and upper bounds such that $u_{\min}u_{\max} < 0$. Furthermore, $a(x) : \mathcal{D} \rightarrow \mathbb{R}^n$ and $b(x) : \mathcal{D} \rightarrow \mathbb{R}^n$ are bounded, uncertain, sufficiently smooth vector fields on \mathcal{D} , that is $a(x), b(x) \in C^\rho$, with ρ being the relative degree determined by the output $y \in \mathbb{R}$. Specifically, the output of the system y is chosen as the function $c(x) \in C^{\rho+1}$ such that the following assumption holds.

Assumption 1 (Relative degree invariance)

System (1) is complete in a region $\mathcal{D}_0 \subset \mathcal{D}$ meaning that $x(t) \in \mathcal{D}_0$ and, for each initial state x_0 and each control u , $x(t)$ is defined for almost all $t \in \mathbb{R}^+$. It has uniform and time-invariant relative degree equal to ρ , with $1 \leq \rho \leq n$, that is $L_b L_a^{i-1} c(x) = 0$, $i = 1, 2, \dots, \rho - 1$ and $L_b L_a^{\rho-1} c(x) \neq 0$, for all $x \in \mathcal{D}_0$. Moreover, it admits a normal form in the region \mathcal{D}_0 .

The applicability of Assumption 1 is determined by the choice of the function $c(x)$ made by the designer (see [18, Section III] for some examples). By virtue of this assumption, there exists a diffeomorphism of the form $\Phi(x) : \mathcal{D}_0 \rightarrow \Phi(\mathcal{D}_0)$, with $\Phi(\mathcal{D}_0) \subset \mathbb{R}^n$, such that

$$\begin{cases} \dot{z} = f_0(z, \sigma) & (3a) \\ z(0) = z_0 & (3b) \\ \dot{\sigma}_i = \sigma_{i+1}, \quad i = 1, \dots, \rho - 1 & (3c) \\ \dot{\sigma}_\rho = f_1(z, \sigma) + f_2(z, \sigma)u & (3d) \\ y = \sigma_1 & (3e) \\ \sigma(0) = \sigma_0. & (3f) \end{cases}$$

Equations (3a)–(3f) are said to be in the *normal form*, which is defined globally if the mapping $\Phi(x)$ is a global diffeomorphism (see [20, Chapter 13] for detailed definitions). In equations (3), $z \in \mathbb{R}^{n-\rho}$ is the state of the internal dynamics, $\sigma := [\sigma_1 \ \sigma_2 \ \dots \ \sigma_\rho]^\top \in \mathbb{R}^\rho$ is the vector of the sliding variable and its derivatives, while $f_1(z, \sigma) = L_a^\rho c(x)$ and $f_2(z, \sigma) = L_b L_a^{\rho-1} c(x)$ are bounded sufficiently smooth uncertain functions. This last property is obtained from system (1). In fact, since a and b are sufficiently smooth bounded functions, and $\Phi(\mathcal{D}_0)$ is a bounded set, vector fields f_1 and f_2 are continuous bounded uncertain functions as well, i.e.,

$$\exists \phi > 0 : |f_1(z, \sigma)| \leq \phi, \forall (z, \sigma) \in \Phi(\mathcal{D}_0) \quad (4)$$

$$\exists \delta > 0 : f_2(z, \sigma) \leq \delta, \forall (z, \sigma) \in \Phi(\mathcal{D}_0) \quad (5)$$

$$\exists \gamma > 0 : f_2(z, \sigma) \geq \gamma, \forall (z, \sigma) \in \Phi(\mathcal{D}_0). \quad (6)$$

Note that, as typically assumed in sliding mode control frameworks, f_2 has known constant sign. However, possible strategies to address the problem of controlling systems with unknown control direction are given for instance in [21–23], among others. Furthermore, since the input saturation, which depends on the nature of the considered plant, has to permit the suppression of the uncertain terms, the following feasibility assumption is required.

Assumption 2 (Bounds feasibility) Given the constraint (2) with $u_{\min}u_{\max} < 0$ and bounds (4) and (6), it must hold

$$\min(|u_{\min}|, |u_{\max}|) > \frac{\phi}{\gamma}. \quad (7)$$

Note that Assumption 2 is instrumental to ensure that the input saturation bounds of the system dominate the worst realization of the uncertain terms, for any possible choice of the initial condition $x_0 \in \mathcal{D}_0$. As a consequence, the designed control input will be capable of attracting the sliding variable towards the corresponding manifold.

Remark 1 (Symmetry of bounds) Note that Assumption 2 is valid for any symmetric and asymmetric bounds with $u_{\min}u_{\max} < 0$. However, in the particular case of systems with input bounds such that $u_{\min}u_{\max} \geq 0$, the input u can be remapped into a new control variable, namely \tilde{u} , given by

$$\tilde{u} = \frac{u - u_{\max}}{u_{\max} - u_{\min}}(\tilde{u}_{\max} - \tilde{u}_{\min}) + \tilde{u}_{\max}, \quad (8)$$

with $\tilde{u}_{\min}, \tilde{u}_{\max}$ arbitrarily chosen scalars such that $\tilde{u}_{\min}\tilde{u}_{\max} < 0$. Such remapping guarantees that the new control variable is bounded as $\tilde{u} \in [\tilde{u}_{\min}, \tilde{u}_{\max}]$. This relationship in turn implies a redefinition of the vector fields f_1 and f_2 as

$$\begin{aligned} \tilde{f}_1(z, \sigma) &= f_1(z, \sigma) + f_2(z, \sigma) \frac{\tilde{u}_{\max}u_{\min} - \tilde{u}_{\min}u_{\max}}{\tilde{u}_{\max} - \tilde{u}_{\min}} \\ \tilde{f}_2(z, \sigma) &= f_2(z, \sigma) \frac{u_{\max} - u_{\min}}{\tilde{u}_{\max} - \tilde{u}_{\min}}, \end{aligned}$$

with new bounds $\tilde{\phi}$ and $\tilde{\gamma}$, respectively. The new formulation is again consistent with Assumption 2.

As for the symmetric case, instead, it directly follows that

$$u_{\max} > \frac{\phi}{\gamma}, \quad (9)$$

with lower bound $u_{\min} = -u_{\max}$. \square

Regarding the choice of the sliding variable in accordance with Assumption 1, the internal dynamics is required to satisfy the following assumption.

Assumption 3 (Zero dynamics) Given the normal form (3), the zero dynamics $\dot{z} = f_0(z, 0)$ is asymptotically stable.

Given the normal form (3a)–(3f), the first control objective is the regulation of the output y to the origin in finite time. Moreover, differently from classical SMC formulations, a continuous input (aimed at chattering alleviation) with a hard constraint on the actuators is required. Notice that a common choice in output-feedback

problems is the selection of the sliding variable σ_1 as the output of the system, namely y , defined as one of the states or as a linear combination of them. This choice is generally considered as part of the design procedure. In this paper we select σ_1 such that the relative degree is equal to ρ , while fulfilling Assumption 1.

4 The Proposed Saturated HOSM Control Law

In this paper, to solve the problem formulated in Section 3, we propose a general approach to design HOSM control strategies combined with an extension of the so-called BIC, exploited in place of the traditional integrator to take into account the input limits.

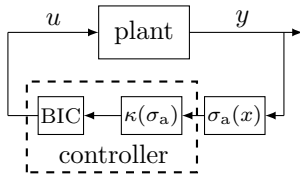


Fig. 1. Representation of the proposed control scheme with HOSM control and BIC mechanism

The considered control scheme in Figure 1 includes three key blocks: the block computing an augmented vector of the sliding variable and its derivatives, namely σ_a defined hereafter, the block containing the discontinuous SMC, and the one with the BIC mechanism. The sliding variable σ_1 is selected equal to the plant output y , while its derivatives are measured or retrieved for instance by the so-called Levant's differentiator of the suitable order [24]. The vector of the sliding variable and its derivatives suitably augmented is then used by the SMC law, which generates a discontinuous signal. The latter is directly transmitted to the BIC block, which sends to the plant a continuous signal fulfilling the hard constraint (2).

Therefore, the SMC law and the BIC mechanism contribute to generate the control variable built as the approximation of the time integral of a discontinuous signal, giving rise to a saturated continuous HOSM control.

4.1 Definition of the augmented system

Having in mind to design HOSM control aimed at chattering alleviation, an integrator dynamics is added to (3c)-(3f) as

$$\begin{cases} \dot{\sigma}_i = \sigma_{i+1}, & i = 1, \dots, r-1 \\ \dot{\sigma}_r = f_3(z, \sigma, u) + f_2(z, \sigma)v, \end{cases} \quad (10)$$

where $v := \dot{u}$ is appointed as the discontinuous control law, such that it holds

$$|v(t)| \leq \alpha, \quad (11)$$

for some $\alpha > 0$ being a design parameter. The increased relative degree instead becomes $r = \rho + 1$ such that the overall augmented vector of the sliding variable and its derivatives is now represented by $\sigma_a := [\sigma^\top \ \sigma_r]^\top \in \mathbb{R}^r$. Moreover, the new drift term is $f_3(z, \sigma, u) = L_a^r c(x)$, while f_2 is determined as in (3). Recalling that condition (2) is required, vector fields f_1 , f_2 and f_3 are continuous functions, and $\Phi(\mathcal{D}_0)$ is a bounded set, one also has that

$$\exists \beta > 0 : |f_3(z, \sigma, u)| \leq \beta, \quad \forall (z, \sigma) \in \Phi(\mathcal{D}_0), \quad \forall u \in \mathcal{U}. \quad (12)$$

Moreover, let the following assumption hold.

Assumption 4 (Control amplitude) *Given the conditions (11)-(12), there exists a positive constant $\lambda < \gamma$ such that the control amplitude upper-bound α satisfies*

$$\alpha > \frac{\beta}{\lambda}. \quad (13)$$

4.2 Definition of the SMC law

Relying on (3)–(12) and Assumptions 1–4, the control problem introduced in Section 3 becomes that of designing a feedback control law

$$u(t) = u(0) + \int_0^t v(\tau) d\tau \quad (14)$$

subject to (2) and such that $\forall x_0 \in \mathcal{D}_0, \exists T \geq 0 : \sigma_a(x(t)) \equiv 0, \forall t \geq T$.

Starting from (10), where the relative degree $r \geq 2$ is assumed to be uniform and time invariant by virtue of Assumption 1, let us introduce a discontinuous function \tilde{v} , given by

$$\tilde{v} = \alpha \kappa(\sigma_a), \quad (15)$$

with $\kappa(\sigma_a)$ being the designed SMC law of order r , and with $\alpha > 0$ being the control amplitude such that $|\tilde{v}| \leq \alpha$. The expression of $\kappa(\sigma_a)$ depends on the arbitrary order r and some examples are the Twisting [10], Sub-optimal [11], Terminal [12], Optimal-reaching [25], and Quasi-continuous SMC [26] algorithms. Note that, the complexity of the manifold grows very fast with the order r , and its design can require exact algebraic or numerical methods, which are beyond the scope of the paper.

Remark 2 (Chattering alleviation) *Replacing the discontinuous input signals with continuous ones is a successful attempt to alleviate chattering in the case of HOSM control algorithms which confine the discontinuity of the input into its time derivative. However, the estimation of chattering features in the case of HOSM is still an open problem. Indeed, the presence of some parasitic dynamics (e.g., delays or hysteresis due to sensors and actuators) can even cause an increase of*

the chattering magnitude. In this work, the property of chattering alleviation of conventional continuous HOSM controllers is preserved. However, the analysis of chattering is beyond the scope of this paper, and we refer to [27, 28] and [29] to deepen this interesting topic. \square

4.3 Design of the BIC desaturation mechanism

In this section the enhanced BIC problem in [8] is presented and recast according to the HOSM formulation. The main idea in [8] is to replicate the traditional integral control with an approximation of an integrator capable of constraining the controller output to a given range of the form $[-u_{\max}, u_{\max}]$, while avoiding the well-known windup problem. In this work, we present a new version of the BIC approach in place of the classical integrator applied downstream of the considered discontinuous law. The proposed BIC add-on to the HOSM controller is then capable of maintaining the control signal in the asymmetric range $[u_{\min}, u_{\max}]$ and performing the integral action with a smaller approximation with respect to the results presented in [8].

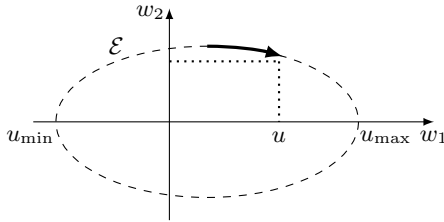


Fig. 2. BIC working principle

Consider the set \mathcal{U} in (2), with bounds $u_{\min} \neq u_{\max}$, and let w_1 and w_2 be additional controller state variables. Consider now the closed curve in Figure 2 represented by the following set

$$\mathcal{E} := \{(w_1, w_2) \in \mathbb{R}^2 : \varepsilon(w_1, w_2) = 0\}, \quad (16)$$

where

$$\varepsilon(w_1, w_2) := \frac{(w_1 - \bar{u})^{2m}}{u^{2m}} + w_2^{2m} - 1 \quad (17)$$

$$\bar{u} := \frac{u_{\max} + u_{\min}}{2}, \quad u := \frac{u_{\max} - u_{\min}}{2}, \quad (18)$$

with $m \in \mathbb{N}$, and $m \geq 1$. In the following, the dependence of ε from (w_1, w_2) will be omitted, for the sake of simplicity. The integration and desaturation strategy, which will be combined with HOSM control laws (15),

instead becomes

$$u = w_1 \quad (19a)$$

$$\begin{bmatrix} \dot{w}_1 \\ \dot{w}_2 \end{bmatrix} = \begin{bmatrix} -k|\varepsilon|^{\frac{1}{2}} & \alpha\kappa(\sigma_a)w_2^{2m-1} \\ -\alpha\kappa(\sigma_a)\frac{w_2}{u^{2m}} & -\frac{k}{u^{2m}}|\varepsilon|^{\frac{1}{2}} \end{bmatrix} \begin{bmatrix} (w_1 - \bar{u})^{2m-1} \\ w_2 \end{bmatrix} \quad (19b)$$

where

$$k := \frac{u^{2m}}{2m} \bar{k}, \quad (20)$$

and $\bar{k} \in \mathbb{R}^+$ is a positive constant gain that regulates the reaching time of the (w_1, w_2) trajectories towards the closed curve $\varepsilon(w_1, w_2) = 0$. Note that, when the trajectories of (w_1, w_2) belong to the closed curve \mathcal{E} , the diagonal terms in (19) are zero and the controller state dynamics are

$$\dot{w}_1 = \alpha\kappa(\sigma_a)w_2^{2m} \quad (21a)$$

$$\dot{w}_2 = -\frac{\alpha\kappa(\sigma_a)}{u^{2m}}w_2(w_1 - \bar{u})^{2m-1}, \quad (21b)$$

where w_2^{2m} can be seen as a nonlinear integrator gain.

4.4 HOSM control embedding BIC mechanism

Before introducing the whole HOSM control combined with the BIC approach, some comments about the gain of the integrator in (21a) are due. When the trajectories of (w_1, w_2) are such that $\varepsilon(w_1, w_2) = 0$, then

$$w_2^{2m} = 1 - \frac{(w_1 - \bar{u})^{2m}}{u^{2m}}. \quad (22)$$

This represents a substantial difference with respect to the BIC formulation in [8], where the integrator gain is

$$w_2^{2m} = 1 - \frac{w_1^2}{u_{\max}^2}, \quad (23)$$

which does not depend on the design parameter m . This implies that, with the new formulation of the BIC, the integral gain will approximate the unit gain as better as the parameter m is increased (see Figure 3, in the case of symmetric saturation bounds for the sake of comparison).

Therefore, for the new formulation of the BIC, for high values of m , the closed curve \mathcal{E} approximates a rectangle, and one has $w_2^{2m} \approx 1$ for almost all values of $w_1 \in [u_{\min}, u_{\max}]$. Hence, the dynamics (19) approximates a pure integrator, i.e., $\dot{w}_1 \approx \alpha\kappa(\sigma_a)$ for almost all $w_1 \in [u_{\min}, u_{\max}]$ (exactly $w_2^{2m} = 1$ for $w_1 = \bar{u}$). More

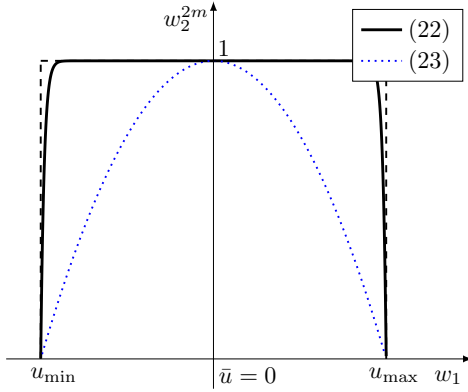


Fig. 3. BIC gain in the proposed extension (solid line) and in [8] (dotted line) in case of $m = 25$, and with symmetric saturation bounds

precisely, substituting (22) into (19), and taking into account (19a), the integral argument in (14) is given by

$$v = \left[1 - \left(\frac{u - \bar{u}}{u} \right)^{2m} \right] \tilde{v}, \quad (24)$$

which represents the proposed general HOSM control law embedding the BIC mechanism. Note that, differently from [7, 8], in this work the BIC strategy is defined for bounds not necessarily symmetric with respect to the w_2 -axis. These bounds are given *a priori* depending on the application. Therefore, the BIC requires the tuning of the sole two parameters k and m . The idea underlying the BIC approach is to make the controller state variables move towards the closed curve (16) and remain on it over time. Indeed, if this is enabled for any initial condition $(w_1(0), w_2(0))$, when w_1 tends to u_{\min} or u_{\max} , then w_2 tends to zero, slowing down the dynamics of w_1 , that is $w_1(t) \in \mathcal{U}, \forall t \geq 0$ (see Figure 2).

Remark 3 (Anti-windup property and tuning)

Note that, differently from the conventional saturated integrator, the BIC strategy has an intrinsic anti-windup property since the integration ‘slows down’ when the input approaches the bound. Analogously, starting from $u \approx u_{\max}$ (or, specularly $u \approx u_{\min}$), the integration also ‘slowly increases’ before w_2^{2m} approaches the value 1.

Regarding the tuning of the parameter $m \geq 1$, a trade-off arises. Lower values of m imply in fact that the integration ‘slows down’ relatively far from the upper and lower limit of the controller output, while enabling an ‘anticipated’ anti-windup effect. Conversely, higher values of m make the integral action very close to the one given by the classical integrator, while yet enabling the anti-windup effect to the close neighbourhoods of u_{\min} and u_{\max} . \square

5 Stability Analysis

In this section, the stability properties of the proposed control strategy are discussed.

5.1 HOSM stability properties

Consider to apply the control law (15) to the normal form (10) (with \tilde{v} in place of v) with bounds given in (5), (6) and (12), so that one obtains the following differential inclusion

$$\begin{cases} \dot{\sigma}_i = \sigma_{i+1}, & i = 1, \dots, r-1 \\ \dot{\sigma}_r \in [-\beta, \beta] + \alpha[\gamma, \delta]\kappa(\sigma_a), \end{cases} \quad (25)$$

or equivalently $\dot{\sigma}_a \in F(\sigma_a)$, with F being a nonempty, closed, convex, locally bounded and upper-semi-continuous vector set. Such a differential inclusion is proved to be a homogeneous Filippov’s inclusion with negative homogeneous degree -1, and the class of considered controllers is defined r -sliding homogeneous (see [30, 31] for further details on homogeneity and finite-time stabilization).

Remark 4 (Homogeneity features of HOSM)

Note that, as proved in [30], almost all known r -sliding controllers, with $r \geq 2$, are r -sliding homogeneous. An exception is instead given by the Terminal algorithms with a specific setting of the control parameters. \square

The following lemma is derived from [30] where homogeneous HOSM laws are discussed and finite-time convergence of trajectories using homogeneity of discontinuous controllers is proved. This significant result is instrumental to prove also the convergence properties of the proposed HOSM control strategy with BIC mechanism.

Lemma 1 (Finite-time convergence [30]) *Let the controllers (15) be r -sliding homogeneous. Then, controllers (15) provide finite-time convergence of each trajectory to the r -sliding mode $\sigma_a \equiv 0$. Moreover, the corresponding Filippov’s inclusion (25) is also globally uniformly finite-time stable.*

PROOF. The proof of the lemma directly follows from [30, Theorem 3] in absence of measurement noises, even including a robust homogeneous differentiator [24] in the control structure.

5.2 BIC stability properties

Now, the following lemma proves that the closed curve (16) is attractive for the BIC state variables (w_1, w_2) , even when the bounds on the input are asymmetric.

Lemma 2 (Stability of the BIC curve) *Given the BIC (19), the curve (16) is almost globally finite-time stable, that is the control output u belongs to the compact interval $[u_{\min}, u_{\max}]$ for any input defined as in (15), and any initial condition $(w_1(0), w_2(0)) \neq (\bar{u}, 0)$.*

PROOF. Consider the Lyapunov function

$$V = \varepsilon(w_1, w_2) + 1 = \frac{(w_1 - \bar{u})^{2m}}{u^{2m}} + w_2^{2m}. \quad (26)$$

Taking the time derivative of V and substituting from (19), it yields

$$\begin{aligned} \dot{V} &= \frac{2m}{u^{2m}} (w_1 - \bar{u})^{2m-1} \dot{w}_1 + 2mw_2^{2m-1} \dot{w}_2 \\ &= -\frac{2m}{u^{2m}} k[\varepsilon]^{\frac{1}{2}} (w_1 - \bar{u})^{2(2m-1)} + \\ &\quad + \alpha\kappa(\sigma_a) \frac{2m}{u^{2m}} w_2^{2m} (w_1 - \bar{u})^{2m-1} + \\ &\quad - \alpha\kappa(\sigma_a) \frac{2m}{u^{2m}} w_2^{2m} (w_1 - \bar{u})^{2m-1} - \frac{2m}{u^{2m}} k[\varepsilon]^{\frac{1}{2}} w_2^{2m} \\ &= -\frac{2m}{u^{2m}} \left((w_1 - \bar{u})^{2(2m-1)} + w_2^{2m} \right) k[\varepsilon]^{\frac{1}{2}}, \quad (27) \end{aligned}$$

which shows that \dot{V} is negative definite outside the closed curve \mathcal{E} , positive inside and zero at the point $(\bar{u}, 0)$. Investigating local dynamics of the equilibrium point $(\bar{u}, 0)$ of system (19), it is an unstable equilibrium point, that is for any $(w_1(0), w_2(0)) \neq (\bar{u}, 0)$, then $(w_1(t), w_2(t)) \neq (\bar{u}, 0)$ for any $t \geq 0$. Hence, the term between brackets in (27) is positive for any $t \geq 0$ as well. Then, choosing the parameter k as in (20) gives

$$\dot{V} = -\bar{k} \left((w_1 - \bar{u})^{2(2m-1)} + w_2^{2m} \right) [V - 1]^{\frac{1}{2}}. \quad (28)$$

Therefore, the Lyapunov function V monotonically tends to 1 in finite time [32]. This in turn implies that, starting from any level set different from $V = 0$ (that is the singleton $(w_1, w_2) = (\bar{u}, 0)$), the Lyapunov function will never assume the value $V = 0$. In other words, the BIC curve \mathcal{E} is almost globally finite-time stable [33, Def. II.1], that is all the trajectories $(w_1(t), w_2(t))$ starting outside or inside the closed curve \mathcal{E} , aside from the point $(\bar{u}, 0)$, will converge towards it in finite time with a rate depending on the gain \bar{k} . The larger the value of \bar{k} , the faster the trajectories $(w_1(t), w_2(t))$ will be attracted to the closed curve \mathcal{E} .

Remark 5 (BIC relationship with HOSM laws)

Note that the proposed version of the BIC algorithm is fed with the discontinuous input (15). It is worth noticing that the Lyapunov function (26) is a Common Lyapunov Function (CLF) [34] for both configurations,

hence such switching input does not affect the stability properties of the exploited BIC method.

Finally, it is worth discussing also some robustness property of the proposed approach in presence of measurement disturbances. Indeed, albeit such disturbances would affect the sliding variable σ , hence the SMC law $\kappa(\sigma_a)$ appearing in (19), these terms do not appear in (26) and (28). Therefore, this means that, for all $(w_1(0), w_2(0))$ different from the unstable equilibrium point $(\bar{u}, 0)$, one will have that $(w_1(t), w_2(t)) \neq (\bar{u}, 0)$ for any $t \geq 0$ despite the presence of measurement disturbances. \square

We prove now that, depending of the sign of the discontinuous input, the lower or upper-bound points $(u_{\min}, 0)$ and $(u_{\max}, 0)$, respectively, are asymptotically stable equilibrium points of (19).

Lemma 3 *Consider the BIC system in (19), and assume that $(w_1(0), w_2(0)) \in \mathcal{E}$. Then, for $\kappa(\sigma_a) > 0$ (resp., $\kappa(\sigma_a) < 0$) the BIC system has an asymptotic equilibrium point in $(u_{\max}, 0)$ (resp., $(u_{\min}, 0)$), with region of attraction equal to $\mathcal{B}^+ := \{w_1 : w_1 > u_{\min}\}$ (resp., $\mathcal{B}^- := \{w_1 : w_1 < u_{\max}\}$).*

PROOF. Since $(w_1(0), w_2(0)) \in \mathcal{E}$, for Lemma 2 one has that $\varepsilon(w_1(t), w_2(t)) = 0, \forall t \geq 0$, which in turn implies (22). Therefore, exploiting (21a) with (22), it results that $(u_{\max}, 0)$ and $(u_{\min}, 0)$ are equilibrium points. The rest of the proof directly follows through graphi-

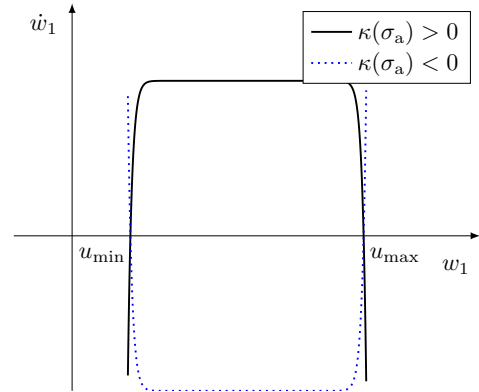


Fig. 4. Representation of relationship (24) when $\kappa(\sigma_a) > 0$ (solid line) and $\kappa(\sigma_a) < 0$ (dotted line)

cal analysis. Consider Figure 4 and the case $\kappa(\sigma_a) > 0$ first. For any $w_1 \in (u_{\min}, u_{\max})$, $\dot{w}_1 > 0$, hence w_1 approaches u_{\max} from the left. Analogously, for any $w_1 \in (u_{\max}, +\infty)$, $\dot{w}_1 < 0$, thus implying again that w_1 approaches u_{\max} from the right. This proves that $(u_{\max}, 0)$ is an asymptotically equilibrium point of (24) for any $w_1 \in \mathcal{B}^+$. The case for $\kappa(\sigma_a) < 0$ is specular, and this concludes the proof.

As a consequence of the previous lemma, the following corollary holds, which is instrumental to prove that the proposed law (24) satisfies condition (11).

Corollary 1 *Consider the BIC system in (19), and assume that $(w_1(0), w_2(0)) \in \mathcal{E}$. If Assumptions 2 and 4 hold with the HOSM control input given by (15), then, there exists $\eta \in \mathbb{R}^+$, such that*

$$\eta \leq \left[1 - \left(\frac{w_1 - \bar{u}}{u} \right)^{2m} \right] \leq 1. \quad (29)$$

PROOF. Consider the HOSM control (15) such that, depending on the initial conditions $\sigma_a(0)$, the sign of $\kappa(\sigma_a)$ is positive (or negative). This means that during the so-called reaching phase $0 \leq t \leq T$, $v(t)$ can be constant equal to α (resp. $-\alpha$) for a sufficiently large time interval that makes $u(t)$ tend to the bounds, according to the BIC action behaving like an integrator. However, it is important to underline that Lemma 3 states that $u(t)$ asymptotically tends to u_{\max} (alternatively, u_{\min}), so that the system cannot exactly reach the saturation. Indeed, Assumption 2 guarantees that there instead exists a constant $\epsilon \in \mathbb{R}^+$ such that the input $u = u_{\max} - \epsilon$ (resp., $u = u_{\min} + \epsilon$) fulfills (7). This implies $\sigma_r > 0$ (resp., $\sigma_r < 0$) and makes the vector field defined by $\dot{\sigma} = f(\sigma)$ always point towards the switching manifold (refer to [14] or [18] for this argument), which means that the sign of $\kappa(\sigma_a)$ changes in finite time, thus desaturating the input. Moreover, the existence of $\epsilon \in \mathbb{R}^+$ determines the existence of η in (29), thus concluding the proof.

5.3 Main result

We are now in a position to introduce the main result.

Theorem 1 (Stability of the controlled system)

Let system (1), with input constraints (2), be controlled via (14) with the HOSM control law (24), and the BIC in (19) having as initial conditions $(w_1(0), w_2(0)) \in \mathcal{E}$. If Assumptions 1–4 hold, then there exists $T \geq 0$ such that $y(t) \equiv 0, \forall t \geq T$. Moreover, $\forall x_0 \in \mathcal{D}_0, x = 0$ is an asymptotically stable equilibrium point of (1), with $u(t) \in \mathcal{U}, \forall t \geq 0$.

PROOF. The proof of the theorem consists of two parts. The first part has in turn to be carried out in two steps. First, it is necessary to prove the finite-time convergence and the feasibility during the reaching phase, that is, given the initial condition $\sigma_a(0)$, the sliding variable and its derivatives are steered to zero in finite time T , while fulfilling the input constraint (2).

Step 1 ($0 \leq t \leq T$): Consider the controlled normal form (10) when the proposed control law (24) with BIC approach is applied, i.e.,

$$\begin{cases} \dot{\sigma}_i = \sigma_{i+1}, & i = 1, \dots, r-1 \\ \dot{\sigma}_r = f_3(z, \sigma, u) + f_2(z, \sigma) \left[1 - \left(\frac{u - \bar{u}}{u} \right)^{2m} \right] \alpha \kappa(\sigma_a). \end{cases} \quad (30)$$

The latter can be rewritten in the following compact form

$$\begin{cases} \dot{\sigma}_i = \sigma_{i+1}, & i = 1, \dots, r-1 \\ \dot{\sigma}_r = f_3(z, \sigma, u) + f_4(z, \sigma, u) \alpha \kappa(\sigma_a), \end{cases} \quad (31)$$

with function f_4 defined as

$$f_4(z, \sigma, u) = f_2(z, \sigma) \left[1 - \left(\frac{u - \bar{u}}{u} \right)^{2m} \right]. \quad (32)$$

Now, given Assumption 1, which implies (3) with f_2 bounded as in (5) and (6), and by virtue of Corollary 1, in Assumption 4 one can pose $\lambda = \gamma\eta$ so that

$$f_4(z, \sigma, u) \leq \delta, \quad \forall (z, \sigma) \in \Phi(\mathcal{D}_0), \forall u \in \mathcal{U} \quad (33)$$

$$f_4(z, \sigma, u) \geq \lambda, \quad \forall (z, \sigma) \in \Phi(\mathcal{D}_0), \forall u \in \mathcal{U}. \quad (34)$$

Therefore, the following differential inclusion can be written:

$$\begin{cases} \dot{\sigma}_i = \sigma_{i+1}, & i = 1, \dots, r-1 \\ \dot{\sigma}_r \in [-\beta, \beta] + \alpha[\lambda, \delta] \kappa(\sigma_a). \end{cases} \quad (35)$$

Since the hypotheses of Lemma 1 are verified even in the case of our HOSM control law embedding the BIC mechanism, there exists $T \geq 0$ such that $\sigma_a(T) \equiv 0$, hence $y(T) = \sigma_1(T) \equiv 0$. Moreover, Corollary 1 ensures that $u(t) \in \mathcal{U}$ in the interval $0 \leq t \leq T$.

After having proved the finite-time convergence of σ_a (consequently also of y) to zero, while fulfilling the input constraint, the second step is to prove that the origin is a uniformly finite-time stable equilibrium point of (10), and the feasibility condition $u(t) \in \mathcal{U}$ is valid also for any $t > T$.

Step 2 ($t > T$): The first result on the uniform stability of $y(t) = 0$ again directly follows from the thesis of Lemma 1, while the feasibility condition can be proved by computing the input when $\sigma_a(t) \equiv 0, \forall t > T$. Since this implies that $\sigma_\rho \equiv 0$, one has $u(t) = -\frac{f_1(z, 0)}{f_2(z, 0)}$. Relying on Assumption 2, it follows that

$$|u(t)| = \frac{|f_1(z, 0)|}{|f_2(z, 0)|} < \frac{\phi}{\gamma} < \min(|u_{\min}|, |u_{\max}|), \quad (36)$$

which in turn ensures that $u(t) \in \mathcal{U}, \forall t \geq 0$.

Finally, as for the second part of the Theorem, exploiting Assumption 3 and inverting the diffeomorphism $\Phi(x)$, according to the reasoning of [20, Chapter 13], then $x = 0$ is an asymptotically stable equilibrium point of (1), with bounded input $u(t) \in \mathcal{U}, \forall t \geq 0$.

Remark 6 (Practices for the controller tuning)

Note that condition (13) in Assumption 4 could be in practice relaxed. Indeed, Assumption 2 allows to make the vector field $\dot{\sigma} = f(\sigma)$ point towards the manifold during the interval when the bounds are approached, in spite of the uncertainties. Far from the saturation limits, instead, the lower bound η in (29) is approximately 1, thus resulting in a greater value of λ in Assumption 4. As a consequence, practically the amplitude α can be less conservative than the theoretical control gain. \square

Relying on Remarks 5 and 6, while the choice of the HOSM controller does not affect the stability of the BIC mechanism, the latter, instead, strictly influences the selection of the HOSM control parameters required to guarantee the stability of the controlled system. However, the general applicability of the proposed BIC add-on is given by the fact that it does not alter in any way the structure of the combined r -order sliding mode controllers.

6 Numerical Example

In this section, the theoretical analysis of the proposed control strategy is assessed in a numerical example.

Consider a controlled Lorenz system, which is a widely known benchmark for its chaotic behavior [35],

$$\begin{cases} \dot{x}_1 &= \theta_1 (x_2 - x_1) \\ \dot{x}_2 &= x_1 (\theta_2 - x_3) - x_2 + u \\ \dot{x}_3 &= x_1 x_2 - \theta_3 x_3, \end{cases} \quad (37)$$

where θ_1 is the so-called Prandtl number, θ_2 is the Rayleigh number and θ_3 is a geometric factor. The control objective is to globally stabilize the system using a bounded control input such that $u \in [u_{\min}, u_{\max}]$. Choosing the output as $y = x_2$, the system has relative degree $\rho = 1$. Hence, a first order sliding mode naturally applies. However, in order to perform a chattering alleviation, a second-order sliding mode control algorithm is selected to control the system with a smooth input by artificially increasing the relative degree to $r = 2$. Therefore, defining the sliding variable as the output, i.e., $\sigma_1 = y = x_2$, the considered diffeomorphism becomes $\Phi(x) = (x_1 \ x_3 \ x_2)^\top = (z_1 \ z_2 \ \sigma_1)^\top$. By deriving the sliding variable and posing $v = \dot{u}$ as the new input, the augmented system (10) starting from (37) can be

written as

$$\begin{cases} \dot{\sigma}_1 = \sigma_2 \\ \dot{\sigma}_2 = -\sigma_2 + (\theta_1 (\theta_2 - z_2) - z_1^2) \sigma_1 + \\ \quad + (\theta_3 z_2 - \theta_1 (\theta_2 - z_2)) z_1 + v \\ \dot{u} = v, \end{cases} \quad (38)$$

that is a relative degree 2 system. The internal dynamics appearing in (3a) is instead $\dot{z}_1 = \theta_1 (\sigma_1 - z_1), \dot{z}_2 = \sigma_1 z_1 - \theta_3 z_2$, with zero dynamics $\dot{z}_1 = -\theta_1 z_1, \dot{z}_2 = -\theta_3 z_2$ being asymptotically stable, as required by Assumption 3. Moreover, the trajectories of the Lorenz system are known to be bounded [35], so that, suitably selecting u_{\min} and u_{\max} , also Assumptions 1 and 2 are satisfied. In the following the system parameters are $\theta_1 = 10, \theta_2 = 28, \theta_3 = \frac{8}{3}$ and the initial condition is $x_0 = [0.16, -0.1, 10.8]^\top$. The asymmetric bounds $u_{\min} = -4, u_{\max} = 3$ satisfy Assumption 2, with uncertainty bounds (4)–(6) equal to $\phi = 2.85$ and $\delta = \gamma = 1$.

First, the proposed control approach with BIC mechanism is applied relying on the original form of Twisting algorithm (briefly, TW in the following). The BIC parameters are selected as $\bar{k} = 10, \alpha = 100, w_1(0) = 2.7$ and $w_2(0)$ such that $(w_1(0), w_2(0)) \in \mathcal{E}$, and $m = 100$ according to Remark 3. According to the TW control, two control parameters, referred to as α_1 and α_2 , are such that the whole control gain dominates $\beta = 45.7$. Specifically, we have selected $\alpha_1 = 1.2$ and $\alpha_2 = 0.8$. In Figure 5 the sliding variable σ_1 and its derivative σ_2 are illustrated along with the continuous input u fed into the plant. It can be observed that, according to Theorem 1, the trajectory is steered to zero in finite time, while the input fulfills the given bounds.

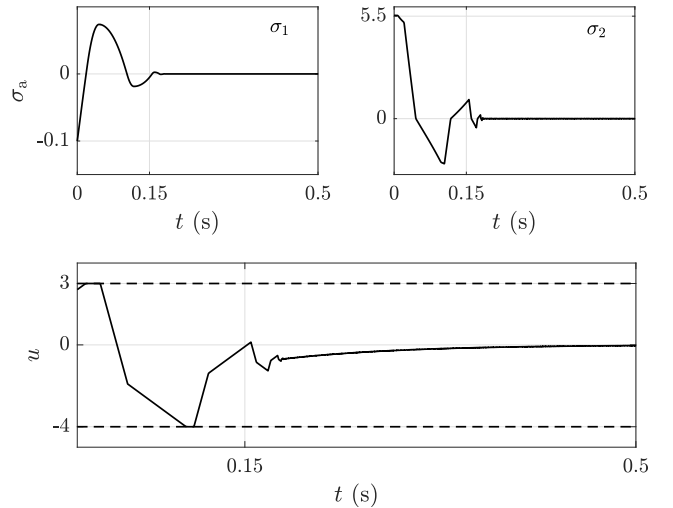


Fig. 5. From the top: time evolution of the sliding variable σ_1 and its derivative σ_2 ; time evolution of the input u when the TW control with BIC is used with asymmetric bounds

In order to further assess the proposal, the previous TW

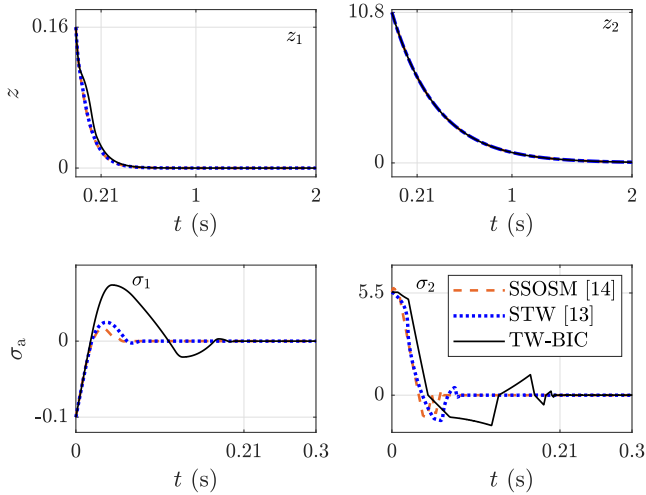


Fig. 6. From the top: time evolution of the internal dynamics z ; time evolution of the sliding variable σ_1 and its derivative σ_2 , when TW with BIC (solid line), SSOSM in [14] (dashed line) and STW in [13] (dotted line) are used

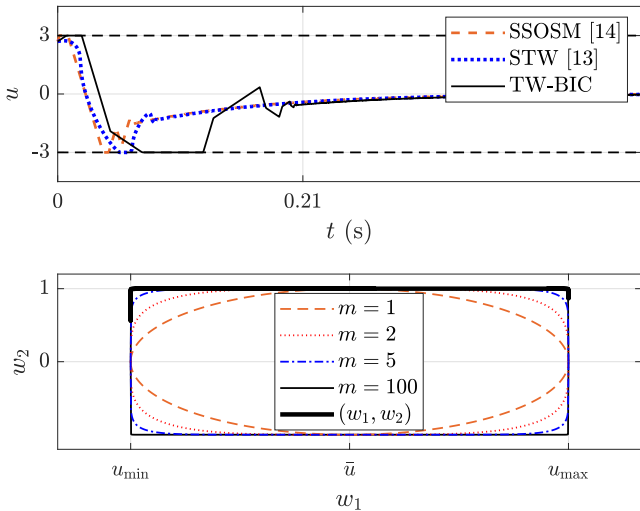


Fig. 7. From the top: time evolution of the input u with bounds when TW with BIC (solid line), SSOSM in [14] (dashed line) and STW in [13] (dotted line) are used; BIC state space $\{w_1, w_2\}$ with $m \in \{1, 2, 5, 100\}$

algorithm combined with BIC is applied in comparison with the modified version of the Suboptimal algorithm (briefly, SSOSM) in [14] and the Super-Twisting (briefly, STW) in [13]. For the sake of a fair comparison, the input bounds are chosen symmetric equal to $u_{\min} = -3$, $u_{\max} = 3$, always satisfying Assumption 2. Referring to the works [14] and [13], the control parameters are set as $\alpha^* = 1$ and $W = 200$ for the SSOSM control, and $k_1 = 10$ and $k_2 = 100$ for the STW approach, respectively. Several properties of the proposed approach can be observed. More specifically, Figure 6 illustrates the time evolution of the internal dynamics which asymptotically converges to zero, according to Assumption 3. In the same figure also the sliding variable and its deriva-

tive, steered to zero in a finite time of $T = 0.21$ s in the proposed case, are illustrated for the three compared controllers. Figure 7 shows instead the evolution of the input u fed into the plant. One observes that the proposed strategy is capable of fulfilling the input constraints. Although the results in terms of convergence time appears different due to the unavoidable different tuning of control gains, we would like to stress that the strategies in [14] and [13] need a modification of the original algorithms, while in our case only the additional BIC mechanism is required, independently of the used HOSM control law. In Figure 7, the BIC phase portrait $\{w_1, w_2\}$ for the considered case study is also reported. Note that the value $m \in \{1, 2, 5, 100\}$ affects the shape of the closed curve \mathcal{E} , thus determining different approximations of the integral action.

7 Conclusions

In this paper we discussed how to recast the so-called BIC approach into the sliding mode control framework in order stabilize nonlinear uncertain systems with saturated actuators via generic continuous HOSM control laws. All the theoretical results have been rigorously proved and assessed in simulations. Future works will be devoted to the control of plants with saturated actuators having unknown bounds of the uncertainties, unknown control direction, and possibly non-minimum phase dynamics.

References

- [1] T. Hu and Z. Lin. *Control Systems with Actuator Saturation: Analysis and Design*. Birkhäuser, Boston, 2001.
- [2] Nguyen H.-N. *Constrained Control of Uncertain, Time-Varying, Discrete-Time Systems. An Interpolation-Based Approach*. Springer International Publishing, London, 2014.
- [3] A. Cavallo, G. Canciello, and A. Russo. Integrated supervised adaptive control for the more electric aircraft. *Automatica*, 117:–, Jul. 2020.
- [4] A. Ferrara, S. Sacone, and S. Siri. *Freeway Traffic Modelling and Control*. Springer International Publishing, Cham, 2018.
- [5] A. Ferrara, G. P. Incremona, and M. Cucuzzella. *Advanced and Optimization Based Sliding Mode Control: Theory and Applications*. Society for Industrial and Applied Mathematics, Philadelphia, 2019.
- [6] P. Hippe. *Windup in Control: Its Effects and Their Prevention*. Springer-Verlag, London, 2006.
- [7] G. C. Konstantopoulos, Q. . Zhong, B. Ren, and M. Krstic. Bounded integral control of input-to-state practically stable nonlinear systems to guarantee closed-loop stability. *IEEE Transactions on Automatic Control*, 61(12):4196–4202, Dec. 2016.
- [8] G. C. Konstantopoulos. Enhanced bounded integral control of input-to-state stable nonlinear systems. *IFAC-PapersOnLine*, 50(1):8151–8156, Jul. 2017. 20th IFAC World Congress.
- [9] V. I. Utkin. *Sliding Modes in Optimization and Control Problems*. Springer Verlag, New York, 1992.

- [10] S. V. Emel'yanov, S. K. Korovin, and A. Levant. High-order sliding modes in control systems. *Computational Mathematics and Modeling*, 7(1):294–318, Jul. 1996.
- [11] G. Bartolini, A. Ferrara, and E. Usai. Chattering avoidance by second-order sliding mode control. *IEEE Transactions on Automatic Control*, 43(2):241–246, Feb. 1998.
- [12] Y. Feng, X. Yu, and Z. Man. Non-singular terminal sliding mode control of rigid manipulators. *Automatica*, 38(12):2159–2167, Dec. 2002.
- [13] R. Seeber and M. Horn. Guaranteeing disturbance rejection and control signal continuity for the saturated super-twisting algorithm. *IEEE Control Systems Letters*, 3(3):715–720, Jul. 2019.
- [14] A. Ferrara and M. Rubagotti. A sub-optimal second order sliding mode controller for systems with saturating actuators. *IEEE Transactions on Automatic Control*, 54(5):1082–1087, May 2009.
- [15] M. Golkani, S. Koch, M. Reichhartinger, M. Horn, and L. Fridman. *Saturated Feedback Control Using Different Higher-Order Sliding-Mode Algorithms*, pages 125–148. Springer International Publishing, Cham, 2020.
- [16] I. Castillo, M. Steinberger, L. Fridman, J. A. Moreno, and M. Horn. Saturated super-twisting algorithm: Lyapunov based approach. In *2016 14th International Workshop on Variable Structure Systems (VSS)*, pages 269–273, Nanjing, China, Jun. 2016.
- [17] R. Seeber and M. Reichhartinger. Conditioned super-twisting algorithm for systems with saturated control action. *Automatica*, 116:–, Jun. 2020.
- [18] G. P. Incremona, M. Rubagotti, and A. Ferrara. Sliding mode control of constrained nonlinear systems. *IEEE Transactions on Automatic Control*, 62(6):2965–2972, Jun. 2017.
- [19] C. Martínez, R. Seeber, L. Fridman, and J. Moreno. Saturated Lipschitz continuous sliding mode controller for perturbed systems with uncertain control coefficient. *IEEE Transactions on Automatic Control*, 66(8):3885–3891, Aug. 2021.
- [20] H. K. Khalil. *Nonlinear Systems*. Prentice Hall, Upper Saddle River, 2002.
- [21] Roger D. Nussbaum. Some remarks on a conjecture in parameter adaptive control. *Systems & Control Letters*, 3(5):243–246, Nov. 1983.
- [22] S. Drakunov. Sliding mode control of the systems with uncertain direction of control vector. In *32nd IEEE Conference on Decision and Control*, volume 3, pages 2477–2478, Dec. 1993.
- [23] G. Bartolini, A. Ferrara, and L. Giacomini. A switching controller for systems with hard uncertainties. *IEEE Transactions on Circuits and Systems I: Fundamental Theory and Applications*, 50(8):984–990, Aug. 2003.
- [24] A. Levant. Higher-order sliding modes, differentiation and output-feedback control. *International Journal of Control*, 76(9–10):924–941, Jan. 2003.
- [25] F. Dinuzzo and A. Ferrara. Higher order sliding mode controllers with optimal reaching. *IEEE Transactions on Automatic Control*, 54(9):2126–2136, Sep. 2009.
- [26] A. Levant. Quasi-continuous high-order sliding-mode controllers. *IEEE Transactions on Automatic Control*, 50(11):1812–1816, Nov. 2005.
- [27] V. I. Utkin. Discussion aspects of high-order sliding mode control. *IEEE Transactions on Automatic Control*, 61(3):829–833, Mar. 2016.
- [28] U. Pérez-Ventura and L. Fridman. When is it reasonable to implement the discontinuous sliding-mode controllers instead of the continuous ones? Frequency domain criteria. *International Journal of Robust and Nonlinear Control*, 29(3):810–828, Jan. 2019.
- [29] C. A. Martínez-Fuentes, U. Pérez-Ventura, and L. Fridman. Chattering analysis for Lipschitz continuous sliding-mode controllers. *International Journal of Robust and Nonlinear Control*, 31(9):3779–3794, Jun. 2020.
- [30] A. Levant. Homogeneity approach to high-order sliding mode design. *Automatica*, 41(5):823–830, May 2005.
- [31] A. Polyakov. *Generalized Homogeneity in Systems and Control*. Communications and Control Engineering. Springer International Publishing, Cham, 2020.
- [32] J. J. E. Slotine and W. Li. *Applied Nonlinear Control*. Prentice Hall, Upper Saddle River, 1991.
- [33] P. Monzón. On necessary conditions for almost global stability. *IEEE Transactions on Automatic Control*, 48(4):631–634, Apr. 2003.
- [34] D. Liberzon. *Switching in Systems and Control*. Systems & Control: Foundations & Applications. Birkhäuser, Boston, 2003.
- [35] Z. Chen and J. Huang. *Stabilization and Regulation of Nonlinear Systems*. Control and Signal Processing. Springer, Cham Heidelberg, 2015.